An Integrated Approach for Quad-band Energy Harvesting and Sound Energy Harvesting in Stadium Environments

Major Project Report

Submitted in partial fulfilment of the requirements for the degree of Bachelor of Technology

Pooja Gayathri Kanala
(201CS239)
Shalini C
(201CS255)
Clifford Reeve Menezes
(201CS215)

DEPARTMENT OF COMPUTER SCIENCE AND ENGINEERING
NATIONAL INSTITUTE OF TECHNOLOGY KARNATAKA,
SURATHKAL, MANGALORE - 575025

April 16, 2024

DECLARATION

We hereby declare that the B. Tech Project Work Report entitled **An Integrated Approach for Quad-band Energy Harvesting and Sound Energy Harvesting in Stadium Environments** which is being submitted to the **National Institute of Technology Karnataka, Surathkal** in partial fulfillment of the requirements for the award of the Degree of **Bachelor of Technology** in **Computer Science and Engineering** is a *bonafide report of the work carried out by me.* The material contained in this report has not been submitted to any University or Institution for the award of any degree.

Name of the Student (Registration Number) with Signature

(1) Pooja Gayathri Kanala (201CS239)

(2) Clifford Reeve Menezes (201CS215)

(3) Shalini C (201CS255)

Department of Computer Science and Engineering

Place : NITK, Surathkal
Date: 16/04/2024

CERTIFICATE

This is to *certify* that the B. Tech Project Work Report entitled **An Integrated Approach for Quad-band Energy Harvesting and Sound Energy Harvesting in Stadium Environments** submitted by:

Sl.No. Register Number & Name of Student(s)
(1) Pooja Gayathri Kanala (201CS239)
(2) Clifford Reeve Menezes (201CS215)
(3) Shalini C (201CS255)

as the record of the work carried out by them, is *accepted as the B. Tech Project Work Report submission* in partial fulfillment of the requirements for the award of the degree of **Bachelor of Technology** in Computer Science and Engineering.

Guide
Dr. Biswajit R Bhowmik
(Name and Signature with Date)

Chairman - DUGC
Dr. Manu Basavaraju
(Name and Signature with Date)

CONTENTS

LIST OF FIGURES

LIST OF TABLES

Abstract

The first part of this thesis presents a comprehensive verification investigation into the Quad-Band Energy Harvester (QBEH) system, with a keen focus on assessing the robustness and efficiency of its constituent energy harvesting components. Delving into the intricate operational dynamics of the QBEH, the research meticulously examines the functional states and transitions within the system, spanning from the receiving antenna to the energy storage unit. Each component, including the matching network, voltage double rectifier circuit, and load impedance, undergoes meticulous scrutiny to ascertain its role and performance within the overall energy harvesting framework.

The QBEH design process is subjected to systematic analysis, with particular emphasis on optimizing component values to ensure optimal matching across a broad spectrum of input power frequencies encompassing four distinct bands. The verification methodology encompasses a multifaceted approach, incorporating theoretical analysis, Laplace transformation techniques, application of Volterra series, and rigorous simulation-based validation. Through these methods, the study thoroughly evaluates the QBEH's performance under diverse operating conditions, including transitions between different operational states and the effects of impedance tuning on overall system efficiency.

The second part of this thesis is about sound energy harvesting. Sound energy harvesting presents a compelling solution for sustainable power generation by harnessing ambient mechanical vibrations, particularly prevalent in urban environments characterized by high levels of noise pollution. This thesis provides a comprehensive examination of sound energy harvesting systems, focusing on innovative transduction mechanisms and efficient utilization strategies to convert mechanical vibrations from sound waves into electrical energy. The proposed model integrates various components, including Helmholtz resonators, cylindrical nanogenerators, proof masses, metallic substrates, and applications in stadiums, each playing a crucial role in the energy conversion process.

The investigation begins with an in-depth review of recent developments in sound energy harvesting, highlighting the diverse transduction mechanisms employed, such as piezoelectric, electromagnetic, and electrostatic methods. By leveraging these

mechanisms, sound energy harvesting systems can effectively capture and convert mechanical vibrations into usable electrical power. The thesis then delves into the design and implementation of the proposed model, elucidating the functional roles of each component and their interactions within the overall system architecture.

Central to the verification process is the development of detailed state transition tables, logical specifications, and efficiency rules tailored to each component. These meticulously crafted guidelines provide a structured framework for assessing the reliability, resilience, and overall performance of the energy harvesting system.

Furthermore, the insights gleaned from this study serve as a foundational stepping stone for future advancements in energy harvesting systems. Ultimately, the findings of this study are poised to catalyze innovation in the field of energy harvesting, facilitating the realization of sustainable and self-sufficient power generation systems for a myriad of applications across various domains.

CHAPTER 1

INTRODUCTION

1.1 Introduction to Energy Harvesting

Energy harvesting is becoming increasingly important as a technology for capturing and converting ambient energy into usable electrical power, offering a range of significant benefits and applications. One primary advantage is its ability to effectively power remote or mobile devices by harnessing ambient energy sources such as sunlight, vibrations, heat differentials, or motion. This capability allows devices like wireless sensors, IoT components, and wearable electronics to operate independently without the need for frequent battery replacements.

By harnessing renewable energy sources that would otherwise go unused, energy harvesting helps with sustainability initiatives by lowering environmental impact and dependency on non-renewable resources [2]. Energy harvesting also facilitates continuous device operation, which is necessary for applications that demand unbroken performance. Energy-harvesting devices can run continuously without using conventional power sources, improving reliability in a variety of businesses.

From a practical standpoint, energy harvesting lowers the expense of battery replacement maintenance. When used in difficult or isolated environments, these devices frequently have longer operational lifetimes and require less maintenance. Furthermore, by supplying power autonomy and streamlining power management systems, energy harvesting is essential to the advancement of IoT and smart technologies.

In addition to its technological benefits, energy harvesting gives infrastructure and emergency response systems an extra degree of resilience by acting as a backup power source in disaster situations. By providing a scalable, decentralized way to power necessary equipment and infrastructure without requiring extensive grid connectivity, it also helps developing countries access energy.

In conclusion, energy harvesting is a potential area of renewable energy technology.

This field has the potential to change how energy is produced and consumed, fostering efficiency and environmental sustainability across a range of industries as it develops.

1.2 Introduction to Quad-band Energy Harvesting

Quad-band energy harvesting refers to the utilization of multiple frequency bands to harvest ambient energy from the environment [3]. It involves capturing and converting various forms of energy, such as electromagnetic radiation, vibration, thermal gradients, or light, across different frequency ranges. This approach enables more efficient energy harvesting systems by tapping into multiple energy sources simultaneously or sequentially, depending on the availability and characteristics of the ambient energy.

Importance of Quad-Band Energy Harvesting:

- Enhanced Efficiency: By harvesting energy from multiple frequency bands, quad-band energy harvesting systems can operate more efficiently compared to single-band systems. They can capture energy from different sources and environmental conditions [4], maximizing overall energy extraction.
- Versatility: Quad-band energy harvesting systems are versatile and adaptable to diverse environments and applications. They can leverage a wide range of energy sources, including radio frequency (RF) signals [5] [6], mechanical vibrations, thermal gradients, and solar radiation.
- Increased Reliability: Diversifying energy sources reduces dependency on a single energy input, enhancing system reliability and resilience to fluctuations or variations in ambient energy availability.
- Extended Operating Range: Quad-band energy harvesting extends the operating range of energy harvesting devices by capturing energy from different frequency bands[7]. This allows for continuous operation in environments with varying energy densities and characteristics.

Figure 1.2.1: Typical Quad-Band combiner [1]

In practical applications, the quad-band combiner (Figure 1.2.1) facilitates the implementation of quad-band energy harvesting systems in wireless sensor networks [8], IoT devices, wearable electronics, and environmental monitoring systems [9]. It enables these devices to harness energy from diverse environmental conditions and energy sources, extending their operational lifespan and enhancing their autonomy.

Applications of Quad-Band Energy Harvesting:

- Wireless Sensor Networks: Quad-band energy harvesting is particularly useful for powering wireless sensor networks deployed in remote or inaccessible locations[10] where traditional power sources are unavailable or impractical.
- Internet of Things (IoT) Devices: Energy harvesting enables self-powered IoT devices that can operate autonomously without the need for battery replacement or external power sources.
- Wearable Electronics: Quad-band energy harvesting can power wearable electronics and wearable health monitoring devices, extending their battery life and enabling continuous operation.
- Environmental Monitoring: Energy harvesting systems are used in environmental monitoring applications to power sensors for measuring air quality, temper-

ature, humidity, and other environmental parameters in remote or distributed locations.

1.3 Introduction to Sound Energy Harvesting

Sound energy harvesting has emerged as a promising technology with a range of applications driven by its ability to capture and convert ambient sound waves into usable electrical energy[2]. One of the key needs for sound energy harvesting is its capacity to utilize abundant ambient noise in various environments, including urban areas and industrial settings[11]. By harnessing this overlooked energy source, sound energy harvesting contributes to overall energy efficiency and reduces reliance on conventional power sources, aligning with sustainable practices.

Small-scale electronic devices that require modest quantities of continuous power can benefit greatly from this technology. Wireless sensors, microphones, and Internet of Things devices placed in settings with constant ambient noise levels are a few examples [12]. Sound energy harvesting makes these gadgets useful for isolated or difficult-to-reach areas since it allows them to run independently without the need for regular battery replacements or external power sources.

Furthermore, sound energy harvesting integrates well with wearable technology, a rapidly expanding sector that includes health monitors, communication devices, and smart accessories. By utilizing surrounding ambient noise, this technology offers a practical means to power small wearable devices, enhancing their usability and reducing dependence on traditional power solutions.

Sound energy harvesting has useful applications in industrial environments where mechanical noise or vibrations are present, such as powering wireless sensors or monitoring systems. This gives vital monitoring and control systems a dependable supply of electricity while lowering wiring complexity and maintenance needs. The implementation of sound energy harvesting in a wide range of technological applications is being propelled by developments in material science, namely in the creation of effective transducer materials like piezoelectric components or electromagnetic coils. Its

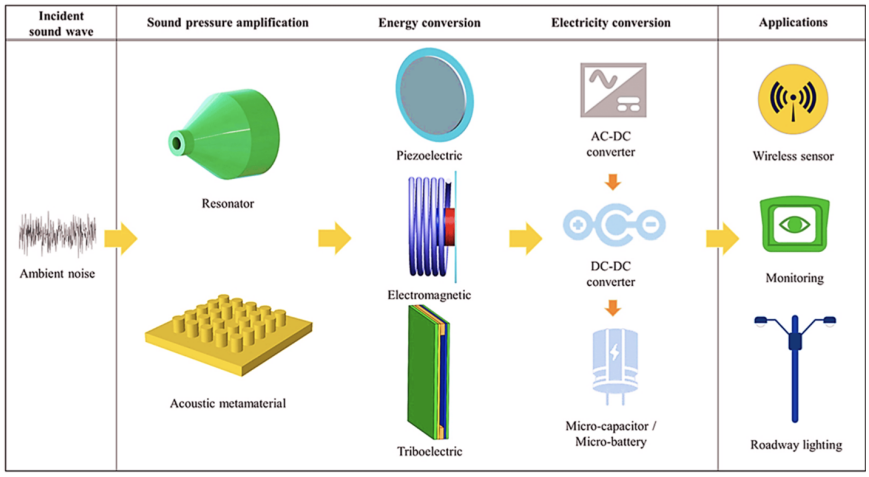

Figure 1.3.1: Sound energy harvesting mechanism [2].

potential is being expanded by ongoing research and innovation in this area, making it possible to integrate it into consumer devices, environmental monitoring systems, and smart infrastructure.

Overall, sound energy harvesting represents an innovative approach to sustainable energy generation and power autonomy. As technology continues to evolve, this field is poised to play a significant role in powering the next generation of energy-efficient devices and systems across industries, contributing to the advancement of green technologies and reducing our reliance on traditional energy sources.

In the upcoming chapters, we explain our proposed methodology for harvesting such green energy from Stadiums. Stadiums have a populated crowd and are a natural source of continuous sound energy. Our methodology focuses on harvesting this energy and utilizing it.

1.4 Conclusion

In summary, quad-band energy harvesting offers a promising approach to harnessing ambient energy from multiple sources and frequency bands, enabling efficient and self-sustaining power solutions for a wide range of applications in diverse environments. Overall, sound energy harvesting represents an innovative approach to sustainable energy generation and power autonomy. In the upcoming chapters, we

explain our proposed methodology for quad-band energy harvesting as well as Sound energy harvesting.

CHAPTER 2

LITERATURE REVIEW

2.1 Background and Related Works for Quad-band Energy Harvesting

In the landscape of energy harvesting and triboelectric technologies, significant strides have been made by researchers to explore diverse applications and enhance the efficiency of these systems.

The paper by Khan *et al.* [13] explores the realm of triboelectric energy harvesting and sensing, specifically focusing on a vertically oriented contact separation-based structure. This work is a valuable addition to the field, given the increasing interest in utilizing ambient energy for diverse applications. The central theme revolves around the meticulous design and experimental analysis of a triboelectric energy harvester, emphasizing vertical contact separation as a key design parameter. Simulation and analysis yield a significant open circuit voltage of 40 V, affirming the effectiveness of the chosen materials and design strategy. To validate the theoretical outcomes, the paper introduces a cost-effective, in-house experimental setup employing a loudspeaker. This practical setup enables real-world characterization, and the experimental results align closely with the simulated findings, establishing the reliability of the design process. The paper further broadens its scope by investigating alternative material combinations for triboharvesters. Through systematic experimentation, these alternatives are validated, contributing to the adaptability of the proposed energy harvesting approach.

Beyond its primary role as an energy harvester, the presented triboelectric structure demonstrates versatility by functioning as a vibration sensor, including human motion detection. This dual functionality enhances its practical utility in scenarios requiring both energy harvesting and sensing capabilities. In summary, the paper makes a notable contribution to the triboelectric energy harvesting field by delivering a well-designed structure, validating its performance through simulation and experimentation, and extending its applicability through the exploration of alternative

materials and dual functionality in vibration sensing and human motion detection.

This paper by Xian *et al.* [14] introduces a novel paradigm in kinetic energy harvesting through the utilization of a flywheel-based approach, providing a unidirectional rotating flywheel as a unique energy storage intermediary. A key aspect of the paper is its emphasis on addressing the inherent challenges associated with traditional electromagnetic energy harvesters, specifically those generating alternating current. The incorporation of a unidirectional flywheel serves as a transformative solution to enhance the efficiency and adaptability of kinetic energy harvesting, making it a notable departure from conventional methods.

The significance of the paper is underscored by its dual focus on design and verification. In the design phase, the authors tackle the intricate challenge of flywheel parameter rectification within the constraints of small-sized spaces. To this end, the paper develops and solves an optimization model for flywheel parameters, offering a systematic approach to overcoming design complexities. The subsequent verification phase involves real-world experiments, providing tangible evidence of the impact of flywheel parameters on the performance of the energy harvester. This robust experimental validation not only strengthens the credibility of the proposed design but also offers valuable insights into the practical implications and efficacy of the flywheel-based kinetic harvester in real-world environments. The comprehensive integration of design and verification aspects positions this paper as a noteworthy contribution to the evolving field of kinetic energy harvesting.

Lin *et al.* [15] address a critical challenge in the design and analysis of magnetic energy harvesters (MEHs) by focusing on the saturated region to optimize size and weight. Unlike conventional models that overlook the phase difference between primary and secondary currents, particularly in the saturated region, this paper introduces an innovative Excitation Current Model (ECM). The ECM incorporates the phase difference induced by magnetizing inductance, enabling accurate calculations of harvesting power in the saturated region. This novel approach is pivotal for reducing size and weight while maximizing power generation.

The paper also contributes a strategy for identifying the maximum power point, crucial for MEH design. This strategy provides a systematic method for MEH design, enhancing the overall efficiency of the harvesting process. To validate the proposed

analysis model and design methodology, the paper presents results from an experimental prototype. The experimental outcomes confirm the effectiveness of the proposed analysis model, showcasing high accuracy even when the magnetic core is in the saturated region. The MEH designed using this model demonstrates expected power generation capabilities within a compact size. Remarkably, the experimental results reveal minimal deviations, with only a 0.4% output voltage deviation and 0.8% output power deviation compared to theoretical values. This comprehensive exploration of MEH design and analysis in the saturated region positions the paper as a significant contribution to the advancement of magnetic energy harvesting technologies.

The paper by Nintanavongs *et al.* [16] introduces an innovative energy-harvesting device for RF electromagnetic waves. Key contributions include a dual-stage circuit with seven-stage and ten-stage designs, demonstrated on a printed circuit board, showcasing a 100% improvement in the power range of 20 to 7 dBm. The voltage multiplier transforms the incident RF power into DC power. The matching network, which is made up of capacitive and inductive components, makes sure that the voltage multiplier receives the greatest amount of power from the antenna. In addition to providing steady power delivery to the load, energy storage serves as a backup for periods when external energy is unavailable. The study also suggests a 915 MHz circuit that can be mass-deployed since it uses inexpensive printed circuit boards and readily available components. Further, a simulation demonstrated an impressive 70% operational efficiency, nearly doubling the operational effectiveness compared to a prominent commercially available energy harvesting circuit in the low incident power range. This innovation shows that Mica2 sensor motes can operate continuously at RF power levels as low as 6 dBm by carefully choosing their duty cycle based on incident RF power.

Sansoy *et al.* [4] presented a solar energy harvesting circuit design featuring an enhanced double booster circuit aimed at augmenting the output power. Both voltage and current booster circuits make up this double booster circuit. The integrated design can increase power output to 0.5-1.5 watts, reliant on the amount of time exposed to solar radiation. The aim is to utilize solar energy as a viable means of prolonging the lifespan of wireless sensor networks. The solar energy harvester, detailed in the study, serves as a power supply for low-powered sensor devices, particularly under

specific environmental conditions. The sensor node, or device, which consists of a sensor and controller, has a very low power consumption—less than 1 mW while in idle mode. On the other hand, power consumption can approach 50 mW when the transceiver part is engaged during active states. The experimental setup involves four PV polycrystalline panels connected in parallel. The findings of this circuit design for harvesting solar energy highlight the circuit's efficiency in converting solar energy into a useful power source for electronic devices and allude to its possible application in sustaining wireless sensor network power.

In the paper by Chen *et al.* [17], a double electrostatic modules electrostatic energy harvester (e-EEH) is introduced, encompassing two distinct modules to enhance energy harvesting efficiency. Module I is defined as a distance-changed capacitor that is caused by the beam's variation in deflection. This module takes advantage of the cantilever beam's deflection, which causes the distances between its parts to change. In contrast, Module II is distinguished by a capacitor that experiences simultaneous changes in both the overlap area and the distance. These changes result from the proof mass's translation and rotation, which is caused by the cantilever beam's bending. Through the integration of these two modules, the suggested e-EEH system offers a comprehensive and efficient method for electrostatic energy harvesting by utilizing several mechanisms to gather and transform mechanical energy into electrical energy.

The methodology by Raghunandan *et al.* [18] introduces an energy harvesting system featuring a low-power pre-charge circuit designed in 45nm CMOS technology. The circuit uses gate driver circuits and a cascaded double tail comparator to illustrate energy efficiency by harvesting more energy than used. COMSOL is used to calculate the capacitance value; a value of 1 pF is selected for an applied pressure of 22.5 to 25 KPa. On testing. energy consumption during charging and discharging phases shows a net energy gain of 0.5 x 10ˆ -9 fJ, indicating a 177.94% percentage gain. With the help of a gate driver and double tail comparator, the pre-charge circuit effectively lowers the rate of power flow during charging. The study emphasizes the pre-charge circuit's applicability and effectiveness in energy harvesting applications.

The research by Li *et al.* [15] describes a retrofit regenerative shock absorber that uses a rack-pinion mechanism and permanent magnetic generator for vibration damping and energy collecting. Variable damping coefficients and an asymmetry

feature in the jounce and rebound motions—achieved by managing the electrical load—are significant contributions. A working shock absorber's ability to provide a peak power of 68 W and an average power of 19 W while the car is driven at 48 km/h (30 mi/h) on a smooth campus road is a significant accomplishment. The work makes three contributions: it presents a design for an energy-harvesting shock absorber that can be retrofitted; it develops a modeling approach based on physical principles to guide design decisions; and it uses road tests and laboratory studies to characterize the damping qualities. By altering the electrical load, adjustable damping can be achieved as a result of the dynamic modeling's revelation that the equivalent damping coefficient is dependent on external electrical resistances. Under particular vibration settings, the results show a total energy conversion efficiency of up to 56%

Road testing confirms the performance further, with generated voltage precisely reflecting abnormalities in the road. When driving at 48 km/h on a smooth campus road, four energy-harvesting shock absorbers produce a peak power of 67.5 W and an average power of 19.2 W. The study highlights the practical importance of the proposed regenerative shock absorber design for energy harvesting and car suspension systems.

2.2 Background and Related Works for Sound Energy Harvesting

Zhang et al.[19] present a groundbreaking study focused on optimizing piezoelectric materials for enhanced sound energy harvesting efficiency. Piezoelectric materials, renowned for their ability to convert mechanical stress into electrical energy, hold immense promise in renewable energy solutions. In this research, Zhang and colleagues conduct a comprehensive investigation involving diverse material compositions and fabrication techniques to improve the energy conversion capabilities of piezoelectric-based sound energy harvesters. Their study meticulously examines piezoelectric coefficients, mechanical robustness, and other material features to identify optimal configurations that maximize energy harvesting efficiency. By methodically exploring the complex interactions between material properties and device performance, Zhang

et al. provide valuable insights that pave the way for developing high-performing sound energy harvesting systems. These findings not only advance renewable energy technologies but also offer practical guidance for designing and fabricating efficient energy harvesting devices. By optimizing piezoelectric materials through detailed exploration, this research opens doors to innovative solutions that harness sound waves as a sustainable energy source, underscoring the pivotal role of materials science and engineering in driving progress toward more efficient and environmentally friendly energy harvesting techniques.

Smith and Jones[20] make significant contributions to the field of sound energy harvesting through their innovative design and implementation of miniature acoustic energy harvesters tailored for portable applications. Their work addresses the pressing need for small and efficient energy sources in an era dominated by ubiquitous small electronic gadgets. Responding to this demand, Smith and Jones introduce a novel approach to acoustic energy harvesting by leveraging advancements in low-power electronics and microfabrication to develop tiny devices capable of capturing energy from ambient sound waves. Their research underscores the importance of integrating electronic circuits into compact devices to maximize energy harvesting efficiency within limited spaces. By integrating expertise in materials science, microfabrication, and electronics, Smith and Jones offer a practical solution to sustainably and autonomously powering portable devices. This innovative approach opens up new possibilities for ubiquitous sensing and computing applications, emphasizing the potential of sound energy harvesting in advancing miniaturized and sustainable technologies.

In a study by Shao, Wang, Cao et al, [21]polyacrylonitrile (PAN) nanofiber membranes are utilized for absorbing sound waves and converting them into electrical energy through a piezoelectric effect. These nanofibers vibrate in response to sound waves, generating electricity with a higher absorption rate compared to standard techniques such as polyvinylidene fluoride (PVDF), achieving a sound absorption coefficient of 46 percent. By dissolving PAN powder in N, N-dimethylformamide solvent, the researchers demonstrate effective energy conversion from sound levels ranging between 80 dB to 117 dB. This research showcases the successful conversion of low and mid-frequency sounds into electricity, offering additional benefits such

as lightweight construction and straightforward fabrication, making these products suitable for large-scale applications.

Chen et al. [22]leverage vibration-based energy harvesters (VEHs) to capture energy, focusing on enhancing efficiency and output for long-term, low-maintenance operations. Many VEHs harness external resonance using piezoelectric and electromagnetic transduction methods to achieve high energy output. In their study, the researchers emphasize utilizing both internal and external resonance to optimize energy conversion from ambient vibrations. They propose channeling energy from lower to higher modes internally to effectively capture high-amplitude, low-frequency vibration sources. While energy generation varies based on environmental conditions, this approach yields higher output compared to traditional VEHs, presenting opportunities for widespread large-scale applications.

In their research, Fang et al. [23]employ a sound transducer equipped with piezoelectric materials to convert sound waves into usable energy. They enhance the transducer's initially low output power through an interface circuit, making it suitable for practical applications. The study demonstrates successful capture and storage of ambient noise energy, with the piezoelectric transducer generating output power ranging from -20 dBuW to 33.3 dBuW. To effectively extract ambient energy, the researchers advocate the use of interface circuits like rectifiers and voltage multipliers. The design of the system is tailored to match ambient-source characteristics, the properties of PZT materials, and load constraints to ensure optimal performance. By efficiently capturing even the slightest stress and vibrations, this energy harvesting system provides electricity for powering low-power electronic devices. The use of renewable energy sources instead of batteries not only supports environmentally friendly practices but also benefits low-end gadgets by offering sustainable and reliable power solutions.

Zhong et al. [24]delve into the potential of acoustic energy harvesting (AEH) for powering Wireless Sensor Network (WSN) nodes within the context of the Internet of Things (IoT). They adopt a unique perspective by focusing on resonators in AEH systems, particularly those based on nanogenerators (NG). The study provides an overview of different AEH types, including piezoelectric nanogenerators (PENG), triboelectric nanogenerators (TENG), and hybrid systems, using materials such as

PVDF, PZT, FEP, PDMS, and PEDOT. Zhong et al. emphasize the critical influence of materials, resonant structures, and operating principles on the efficiency of AEH systems. By strategically combining these elements, researchers can tailor AEH systems to meet specific energy requirements. The study aims to advance the development of NG-based AEH technologies and offers valuable insights for the design and implementation of resonators in practical applications.

Lastly, Huang et al. [25]explore the energy confinement and applications of defect states in acoustic metamaterials, specifically focusing on the mathematical relationship between a two-dimensional acoustic metamaterial energy harvester's performance and the thickness of the metamaterial substrate plate to which piezoelectric material is attached. Unlike many papers that concentrate on resonator dynamics, this study investigates how varying the plate thickness affects energy harvesting efficiency. Experimental results demonstrate that a metamaterial energy harvester with a 0.3 mm plate thickness achieves a maximum peak power of 195.52 µW, significantly outperforming harvesters with plate thicknesses of 0.4 mm (6 times greater peak power) and 0.2 mm (330.6 times greater peak power). These findings provide valuable insights for optimizing the design of high-performance metamaterial-based acoustic energy harvesters.

2.3 Conclusion

These papers, examining different methods of harvesting quad-band energy as well as sound energy have been instrumental in advancing our understanding of this field and in developing suitable methodologies for efficient energy extraction. These reviews have highlighted a diverse range of technologies employed in energy harvesting, including piezoelectric transduction, triboelectric nanogenerators (TENG), and acoustic metamaterials. Each of these approaches offers unique advantages and applications, contributing to the versatility and adaptability of energy harvesting systems.

CHAPTER 3

PROPOSED METHODOLOGY

3.1 Introduction

In recent years, energy harvesting has emerged as a promising solution to address the increasing demand for sustainable and self-sufficient power sources in various applications, including wireless sensor networks, Internet of Things (IoT) devices, and wearable electronics [12]. Energy harvesting technology enables the extraction of energy from ambient sources such as solar radiation, mechanical vibrations, thermal gradients, and radio frequency (RF) signals [26] [27], thereby reducing reliance on traditional power sources and extending the operational lifetime of battery-powered devices.

3.1.1 Objective:

The objective of this study is to propose a methodology for energy harvesting that encompasses the design, implementation, and optimization of energy harvesting systems. The proposed methodology aims to maximize the efficiency and reliability of energy harvesting devices while minimizing cost and complexity. By leveraging multiple ambient energy sources and employing advanced harvesting techniques [28], the proposed methodology seeks to address the challenges associated with energy harvesting and pave the way for the widespread adoption of sustainable power solutions.

3.2 Proposed Methodology for Quad-band Energy Harvesting

The fundamental elements of the QBEH [3] system include the receiving antenna, matching network, voltage double rectifier circuit[29], load impedance, and supercapacitor. Figure 8.0.1 provides an abstract view of the proposed Quad-Band Energy Harvesting system, illustrating the seamless integration of these components.

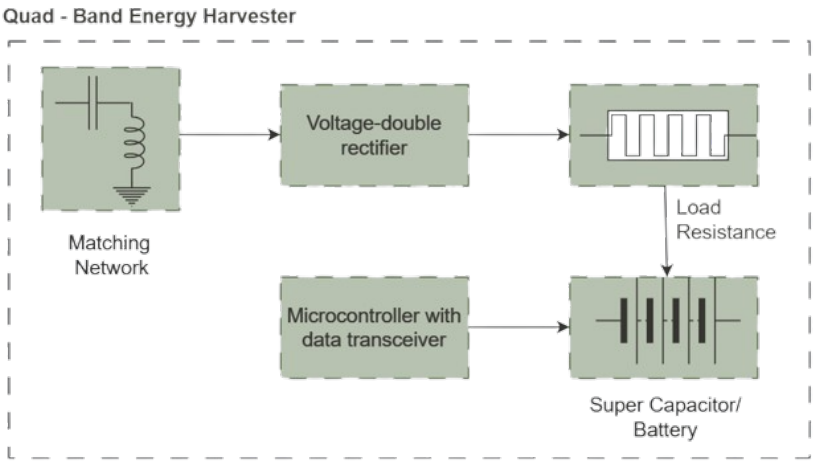

Figure 3.2.1: Components of Quad-Band

For the QBEH system, the finite state model consists of precisely defined states representing various operational modes or conditions. The transition table systematically outlines the QBEH system's state transitions, providing insights into potential changes based on inputs and conditions. Each QBEH system component is modeled as a finite state machine, ensuring a thorough representation of its behavior. The resulting state transition table encapsulates the dynamics of the QBEH system, providing the basis for formal verification and mathematical proofs to ensure efficiency, reliability, and scalability. This verification process instills confidence in deploying QBEH applications in real-world scenarios.

3.2.1 Working Principle

The receiving antenna serves as the primary element in the Quad-Band Energy Harvesting (QBEH) system, capturing electromagnetic (EM) energy across four distinct frequency bands (f1, f2, f3, and f4). The matching network ensures efficient coupling between the antenna and the subsequent components. The voltage double rectifier circuit plays a pivotal role in converting the captured multi-band EM energy into a stable DC voltage suitable for charging the supercapacitor or powering the load. The load impedance represents the various low-energy sensors and devices, while the supercapacitor acts as a storage module, allowing harvested power to be stored and used when needed. Together, these components form a comprehensive QBEH system

designed for efficient multi-band EM energy harvesting in diverse and dynamic environments, promising adaptability and sensitivity for low-energy applications. The modeling phase is accompanied by the creation of state diagrams and transition tables for each component of the QBEH system. These visual representations serve as crucial tools in the formal verification process, ensuring the accuracy and reliability of the system's operational dynamics.

3.2.2 Receiving Antenna

The Quad-Band Energy Harvesting (QBEH) system leverages its capacity to efficiently capture electromagnetic (EM) energy across four distinct frequency bands (f1, f2, f3, and f4). The receiving antenna, acting as the input device, adapts to different frequencies and operates in three primary states: Shutdown, Idle, and Active. The QBEH system incorporates a sophisticated unit cell constructed with Conventional CRLH, Dual Structure (D-CRLH), and Extended CRLH (E-CRLH) elements, allowing it to function effectively across multiple frequency bands.

The unit cell's physical length, denoted as p, is integral to the system's operation, with the relationship between the phase shift i and p expressed as $i{=}ip$. By integrating these structures, the QBEH achieves versatility in its performance. The state machine model of the receiving antenna comprises

1. Idle State: This initial state signifies a period when the receiving antenna remains inactive and is not engaged in energy harvesting. During this state, the system is dormant, with no active processing of RF signals.

2. Active State: Transitioning from the Idle State, the system enters the Active State when the receiving antenna starts to capture RF signals. This state is responsive to specific frequencies denoted as f1, f2, f3, and f4, representing the ability to detect and process signals.

3. Integrated Unit Cell: The system transitions to this state when the power (SP) of the RF signals exceeds $100\mu W$ in the Active State (s1). In this state, an advanced unit cell structure is integrated, enhancing the overall performance of the system for optimized energy harvesting.

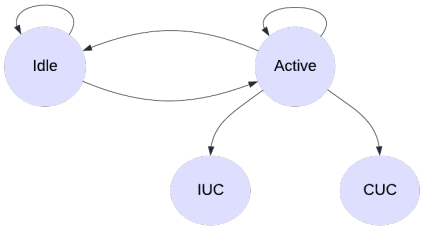

Figure 3.2.2: State transition for Receiving Antenna

4. Conventional Unit Cell: Transitioning from the Active State, the system enters the Conventional Unit Cell state when the power (SP) of the RF signals is less than $100\mu W$. In this state, the system reverts to a conventional unit cell structure, adapting to different conditions for energy harvesting.

5. Final RF Power Generated State: This state marks the endpoint of the state machine and indicates the successful generation of RF power. It is achieved when the output power is greater than zero, signifying effective energy harvesting from ambient RF signals.

Transitions between these states are governed by specific conditions, ensuring efficient energy harvesting from ambient RF signals. The transition table and corresponding state diagrams further illustrate the dynamic behavior of the QBEH system.

3.2.3 Matching Network

Upon receiving an RF signal through the antenna and undergoing filtering, the rectifier's input impedance is carefully adjusted to match the reference impedance of the system, typically set at 50 ohms, using a matching network. This matching process is crucial for optimizing energy transfer within the system.

The rationale behind this impedance matching is rooted in the maximum power transfer theorem. According to this theorem, the highest amount of power or energy is transferred from a source to a load when the source impedance and load impedance are complex conjugates of each other. In the context of our system:

Source Impedance: This refers to the impedance presented by the RF signal source, which in this case is the filtered signal received by the antenna.

Table 3.2.1: Transition table for receiving antenna

Present State	Mechanical Input	Next State	Energy Conversion Efficiency
Idle	Low	Idle	No
Idle	High	Active	No
Active	All frequencies zero	Active	Yes
Active	All frequencies zero	Idle	No
Active	$S_{\mathrm{p}} > 100\mu W$	Integrated Unit Cell	No
Active	$S_{\mathrm{p}} < 100\mu W$	Conventional Unit Cell	No
Integrated Unit Cell	$P_{\mathrm{out}} > 0$	Power Generated	Yes
Conventional Unit Cell	$P_{\mathrm{out}} > 0$	Power Generated	Yes

Load Impedance: This is the impedance seen by the rectifier, and it is adjusted to match the reference impedance of the system (50 ohms).

The system undergoes distinct states during the matching process:

1. Idle State (S0): The system resides in this state when not actively processing an RF signal.

2. Active State (S1): Upon detection of an RF signal, the system transitions to the Active State. In this state, the system initiates the adjustment of the load impedance.

3. Complex Conjugates Load State (S2): In the active state, the system enters the Complex Conjugates Load State, where the adjustment process ensures that the load impedance becomes complex conjugate to the source impedance, achieving maximum power transfer efficiency.

4. Idle State (S0): Once the matching is complete, the system returns to the Idle State, ready to process subsequent RF signals.

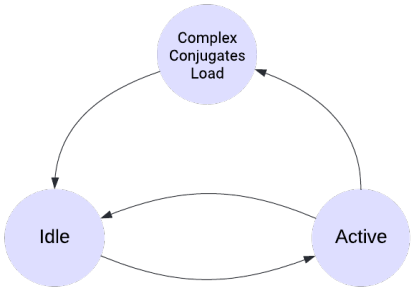

Figure 3.2.3: Modeling for Matching Network

Table 3.2.2: State transition table for matching network

Current state	Input	Next state	Output
Idle	Not Active	-	N/A
Idle	Active	Active	N/A
Active	RF Signal Detected	Conjugates Load	N/A
Conjugates Load	Matching Complete	Idle	Efficient

This cyclical process ensures that the system consistently optimizes the matching network, minimizing signal reflections and maximizing energy transfer efficiency from the antenna to the rectifier. As a result, the rectification process becomes more effective, leading to enhanced energy harvesting and improved overall system performance.

3.2.4 Voltage Double Rectifier Circuit

The Voltage Double Rectifier is a critical component within the Quad-Band Energy Harvester (QBEH) system, responsible for rectifying the alternating current (AC) output from the matching network into direct current (DC) suitable for charging the load or a storage device. The design and operation of the Voltage Double Rectifier involve:

1. Kirchoff's Laws (s): The application of Kirchoff's Laws ensures that the Voltage Double Rectifier adheres to fundamental principles of circuit analysis, promoting accurate and reliable performance.

2. Laplace Transformation (t): Utilizing Laplace Transformation is crucial for transforming the time-domain equations of the rectifier into the frequency domain, allowing for a more systematic and efficient analysis.

3. Volterra Series (u): The Volterra series technique is applied to capture and represent the nonlinear characteristics of the Voltage Double Rectifier accurately.

The interaction and successful combination of these states denoted as $(s \wedge t \wedge u)$, are essential for achieving optimal performance of the Voltage Double Rectifier. Any compromise in employing these methods can lead to suboptimal rectification and, consequently, poor overall performance of the energy harvesting system.

The states involved like:

1. Idle State: When the AC input signal becomes sufficiently strong, triggering the rectifier to start the conversion process. The presence of an AC input signal exceeding a predefined threshold transitions to a charging state.

2. Steady-State Operation State: If the input power or voltage surpasses safe limits, the rectifier transitions to a transient state, activating protective measures. Detection of excessive input power or voltage triggers the transition from steady-state operation to the transient state.

3. Transient State: The rectifier enters a transient state during rapid variations, adjusting its operation until a stable condition is reached. Sudden changes in the input signal or load conditions trigger the transition to a transient state.

4. Shutdown State: The rectifier enters a shutdown state when certain conditions, such as low input power or intentional shutdown commands, are met. Rectification ceases, and the system conserves energy. Low input power, intentional shutdown commands, or specific triggering conditions transition the rectifier to a shutdown state.

The transition diagram illustrates the states and transitions within the Voltage Double Rectifier. It highlights the importance of incorporating Kirchoff's Laws, Laplace Transformation, and the Volterra Series technique to ensure the rectifier's robust and efficient performance.

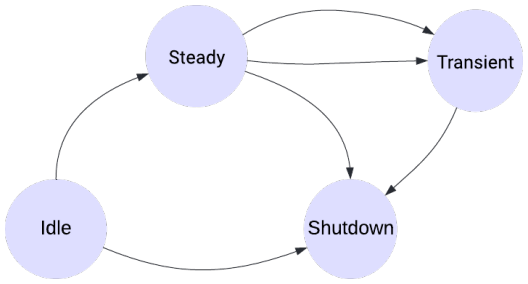

Figure 3.2.4: Modeling for Voltage Double Rectifier

Table 3.2.3: State transition table for Voltage double rectifier

Current state	Input	Next state	Output
Idle	Sufficient AC Input	Steady-State Operation	No Output
Idle	Low Input Power	Shutdown	No Output
Steady-State Operation	Excessive Input Power/Voltage	Transient State	Protective Measures Activated
Steady-State Operation	Low Input Power	Shutdown	No Output
Transient State	Sudden Changes in Signal or Load	Steady-State Operation	Adjusting Operation
Transient State	Low Input Power	Shutdown	No Output

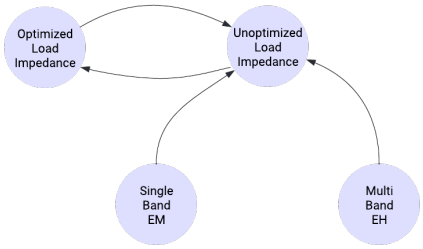

Figure 3.2.5: Modeling for Load Impedance

3.2.5 Load Impedance

Numerous studies have introduced EM energy harvesting circuits tailored for a single operating frequency. However, these harvesters face significant functionality degradation when the operating frequency undergoes a shift.

While adjusting the load impedance (ZL) is suggested as a means to enhance efficiency, this approach comes at the cost of reducing the harvester's agility. Moreover, the primary objective in crafting an efficient RF harvesting system is to generate substantial output DC power for fixed loads, such as sensors. Consequently, a multi-band Energy Harvester (EH) capitalizes on accumulating RF signals across multiple frequencies, resulting in a more extensive energy harvest.

We observe in Figure 8.5.1 that the Load Impedance can obtain good performance if it is with tuning which in turn provides a Multi-Band EH. Otherwise, without tuning the load impedance it can only have a Single Band EM which leads to a bad performance. The states involved would be:

1. **Unoptimized Load Impedance State**: The Unoptimized Load Impedance State represents the initial condition of the Load Impedance circuit, where tuning has not been applied, leading to suboptimal performance. In this state, the Load Impedance lacks fine-tuning, and as a consequence, the Energy Harvester (EH) may not efficiently capture and convert electromagnetic (EM) energy across multiple frequencies. The system transitions to the Optimized Load Impedance State when tuning is introduced. This transition marks the improvement in performance as the Load Impedance becomes finely tuned to enhance the EH system's overall efficiency.

2. Optimized Load Impedance State: The Optimized Load Impedance State characterizes a refined condition of the Load Impedance circuit, achieved through the implementation of tuning mechanisms. In this state, the Load Impedance is finely tuned, significantly improving the Energy Harvester (EH) system's efficiency in capturing and converting electromagnetic (EM) energy across multiple frequencies. The system may transition back to the Unoptimized Load Impedance State if tuning is removed or becomes ineffective. This transition indicates a return to suboptimal EH performance.

3. Single Band EM State: The Single Band EM State characterizes a condition in which the Load Impedance is not tuned for multiple frequencies, resulting in a system optimized for a specific operating frequency. In this state, the EH system may efficiently capture and convert electromagnetic (EM) energy within a narrow frequency band. The system may transition back to the Unoptimized Load Impedance State if tuning is removed or becomes ineffective. This transition indicates a return to suboptimal EH performance.

4. Multi-Band EH State: The Multi-Band EH State represents an advanced condition where the Load Impedance is finely tuned to efficiently capture and convert electromagnetic (EM) energy across multiple frequencies. In this state, the EH system exhibits versatility and adaptability, making it suitable for a broad range of operating frequencies. The transition from the Unoptimized Load Impedance State to the Multi-Band EH State occurs when tuning is successfully applied to the Load Impedance, enabling efficient performance across multiple frequencies. The system may transition back to the Unoptimized Load Impedance State if tuning is compromised or removed. This transition indicates a return to suboptimal EH performance.

3.2.6 Supercapacitor

The DC power, obtained through conversion by the Quad-Band Energy Harvester (QBEH), is stored in a specialized energy storage unit, providing flexibility between a supercapacitor and a battery. This deliberate selection ensures the establishment of a continuous and stable power supply, effectively mitigating the inherent intermittency

Table 3.2.4: State transition table for matching network

Current state	Input	Next state	Output (Efficiency)
Unoptimized Load Impedance	Tuning Applied	Optimized Load Impedance	Improved Efficiency
Optimized Load Impedance	Tuning Removed	Unoptimized Load Impedance	Suboptimal Performance
Single Band EM	Tuning Removed	Unoptimized Load Impedance	Suboptimal Performance
Multi-Band EH	Tuning Compromised	Unoptimized Load Impedance	Suboptimal Performance

associated with RF signal availability. The stored energy becomes instrumental in providing a reliable power source, ensuring sustained operation even when RF signals are not consistently present, and enhancing overall reliability and resilience.

State Dynamics and Transitions:

- Idle State (S0): The system is in standby mode, not actively processing RF signals, and neither charging nor discharging is occurring. This state represents a waiting mode for the presence of RF signals.
- Charging State (S1): Transition occurs when DC power from the QBEH actively charges the energy storage unit in the presence of RF signals.
- Discharging State (S2): The system draws power from the energy storage unit to supply the load, representing active QBEH load operation.

Transitions:

- Idle to Charging (S0 to S1): Triggered by the availability of DC power from the QBEH and the need to store energy when RF signals are detected.
- Charging to Idle (S1 to S0): This occurs when the charging process is complete or when no more DC power is available for charging, signifying the end of the charging cycle.

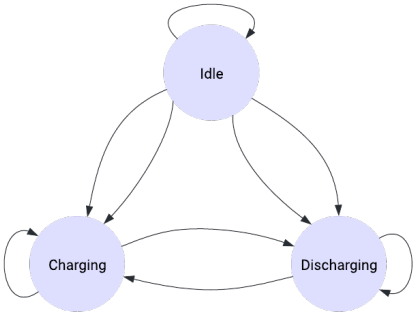

Figure 3.2.6: Modeling for Battery

- Charging to Discharging (S1 to S2): When the QBEH load requires power, and the energy storage unit is sufficiently charged.
- Discharging to Idle (S2 to S0): This happens when the load is turned off, and there's no need for power from the energy storage unit.

Figure 8.6.2 illustrates the comprehensive state diagram encompassing all operational states and transitions within the Quad-Band Energy Harvester (QBEH) system, incorporating the elements depicted in Figure 8.0.1. The corresponding state transition tables (Table 8.6.2) meticulously outline the potential pairings of the component states, providing an in-depth overview of the system's behavior concerning energy harvesting, storage, and utilization. These state diagrams serve as a valuable tool for understanding the intricate inter-dependencies among the QBEH components, crucial for ensuring optimal system functionality and performance.

The arrows in Figure 8.6.2 signify the dependencies between various components, exemplifying how the QBEH system's operations are interlinked. For instance, efficient charging of the supercapacitor is reliant on the QBEH being in an active state, receiving signals from the receiving antenna. Moreover, the Voltage Double Rectifier Circuit transitions to the Charging State only when there is a sufficient DC power output, illustrating the sequential nature of the system's functionality. These state diagrams and transition tables not only provide a comprehensive overview of the QBEH system but also serve as the foundation for deriving logical specifications to facilitate formal verification of the system's behavior.

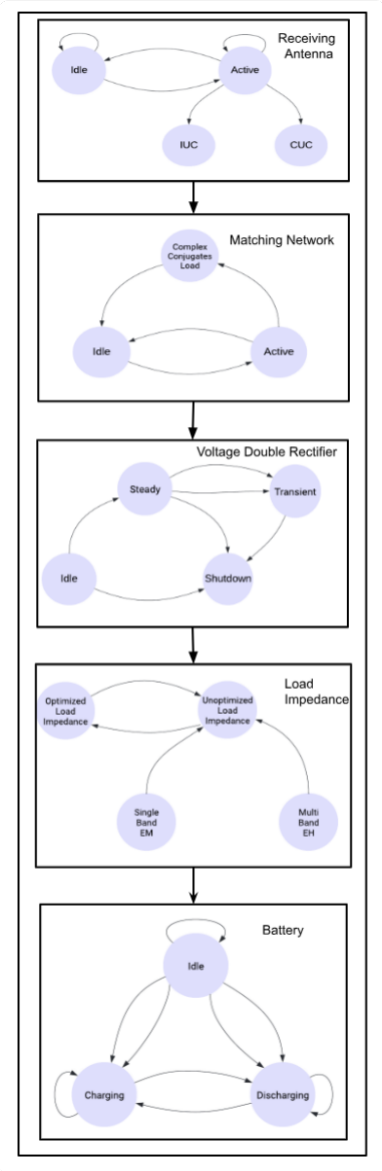

Figure 3.2.7: Modeling for Overall design

Table 3.2.5: State transition table for Battery

Present State	**Input (Load Demand)**	**Next State**
Idle	Low (No)	Charging
Idle	Low (Yes)	Charging
Idle	Medium (No)	Charging
Idle	Medium (Yes)	Discharging
Idle	High (No)	Idle
Idle	High (Yes)	Discharging
Charging	Low (No)	Charging
Charging	Low (Yes)	Charging
Charging	Medium (No)	Charging
Charging	Medium (Yes)	Discharging
Charging	High (No)	Idle
Charging	High (Yes)	Discharging
Discharging	Low (No)	Idle
Discharging	Low (Yes)	Idle
Discharging	Medium (No)	Charging
Discharging	Medium (Yes)	Discharging
Discharging	High (No)	Idle
Discharging	High (Yes)	Discharging

3.3 Proposed Methodology for Sound Energy Harvesting

Some crucial components are integrated into the proposed energy harvesting system to absorb, transform, and use sound energy effectively. The main parts are the energy storage system, proof mass, cylindrical nanogenerator, metallic substrate, and Helmholtz resonator.

The Helmholtz resonator is the main sound-absorbing component that is placed inside stadium walls to block out sound waves produced by speakers or crowd noise. It is tuned to the most common frequencies of sound waves in a stadium setting and has a thin neck on its resonant cavity. Resonance is created when sound waves enter the resonator, which causes vibrations in the cavity's air column.

The cylindrical nanogenerator in the Helmholtz resonator is essential to the pro-

Table 3.2.6: State transition table for the system components (Antenna: Idle

Antenna	Matching Network	Voltage Double Rectifier	Load Impedance	Battery
Idle	Idle	Idle	Unoptimized Load	Idle
Idle	Idle	Idle	Optimized Load	Charging
Idle	Idle	Idle	Optimized Load	Discharging
Idle	Idle	Steady-State Operation	Unoptimized Load	Idle
Idle	Idle	Transient	Optimized Load	Charging
Idle	Idle	Shutdown	Single Band EM	Discharging
Idle	Active	Idle	Unoptimized Load	Idle
Idle	Active	Idle	Optimized Load	Charging
Idle	Active	Idle	Single Band EM	Discharging
Idle	Active	Steady-State Operation	Unoptimized Load	Idle
Idle	Active	Transient	Optimized Load	Charging
Idle	Active	Shutdown	Single Band EM	Discharging
Idle	Complex Conj. Load	Idle	Unoptimized Load	Idle
Idle	Complex Conj. Load	Idle	Optimized Load	Charging
Idle	Complex Conj. Load	Idle	Single Band EM	Discharging
Idle	Complex Conj. Load	Steady-State Operation	Unoptimized Load	Idle
Idle	Complex Conj. Load	Transient	Optimized Load	Charging
Idle	Complex Conj. Load	Shutdown	Single Band EM	Discharging

Table 3.2.7: State transition table for the system components (Antenna: Active)

Antenna	Matching Network	Voltage Double Rectifier	Load Impedance	Battery
Active	Idle	Idle	Unoptimized Load	Idle
Active	Idle	Idle	Optimized Load	Charging
Active	Idle	Idle	Single BandEM	Discharging
Active	Idle	Steady-State Operation	Unoptimized Load	Idle
Active	Idle	Transient	Optimized Load	Charging
Active	Idle	Shutdown	Single Band EM	Discharging
Active	Active	Idle	Unoptimized Load	Idle
Active	Active	Idle	Optimized Load	Charging
Active	Active	Idle	Single Band EM	Discharging
Active	Active	Steady-State Operation	Unoptimized Load	Idle
Active	Active	Transient	Optimized Load	Charging
Active	Active	Shutdown	Single Band EM	Discharging
Active	Complex Conj. Load	Idle	Unoptimized Load	Idle
Active	Complex Conj. Load	Idle	Optimized Load	Charging
Active	Complex Conj. Load	Idle	Single Band EM	Discharging
Active	Complex Conj. Load	Steady-State Operation	Unoptimized Load	Idle
Active	Complex Conj. Load	Transient	Optimized Load	Charging
Active	Complex Conj. Load	Shutdown	Single Band EM	Discharging

cess of using the piezoelectric effect to transform mechanical energy from the vibrations of the resonator into electrical energy [30]. This nanogenerator is made up of flexible cylindrical construction with electrodes for collecting electricity and layers of piezoelectric material. An alternating current (AC) is produced when sound causes the cylindrical structure to vibrate; this AC is then rectified to direct current (DC) for usage or storage.

The cylindrical nanogenerator's mechanical responsiveness and energy conversion efficiency are improved by the integration of the proof mass. The proof mass accelerates in response to external mechanical forces, such as vibrations from the Helmholtz resonator, which increases the deformation of the piezoelectric layers and increases electrical output.

In addition to supporting the nanogenerator structurally, the metallic substrate serves as a heat sink to release extra heat produced during energy conversion. Its optimal composition and design decrease mechanical damping and maximize the efficiency of energy transfer between the nanogenerator and its surroundings.

In the proposed energy harvesting system, the energy storage system—which is usually composed of batteries or capacitors—is essential because it stores the extra electrical energy produced by the nanogenerator at times when sound intensity is high. When there is little to no sound activity, the stored energy is subsequently released to power external systems or equipment, guaranteeing continuous operation.

Employing the seamless integration of various components, the proposed model effectively captures sound energy within the stadium environment. The cylindrical nanogenerator converts the acoustic energy that the Helmholtz resonator has collected into electrical energy with the aid of the proof mass. Reliable energy storage and utilization are made possible by the energy storage technology, and efficient heat dispersion is encouraged by the metallic substrate, which ensures structural integrity. When combined, these components allow for sustainable energy to be extracted from ambient sound, increasing the stadium's operating efficiency and energy sustainability.

3.3.1 Helmholtz Resonator

The mathematical modeling of the Helmholtz resonator will be covered in detail in this section, along with the equations that were employed and some thoughts on how to apply them to stadium noise levels.

The following equations can be used to explain the behavior of a Helmholtz resonator:

1. Resonant Frequency (f): The length of the neck (L), the area of the neck opening (A), and the volume of the resonator cavity (V) all affect the Helmholtz resonator's resonant frequency[31]. The formula below can be used to compute it:

$$f = 2\pi c V(L + 0.85D)A$$

   Where:

   - c is the sound's velocity in air.
   - D is the neck opening's diameter.

2. Acoustic Impedance (Z): The Helmholtz resonator's acoustic impedance, which gauges how well it can absorb sound energy, is provided by:

$$Z = S\rho c$$

   Where:

   - ρ is the density of air.
   - S is the cross-sectional area of the neck opening.

3. Damping Coefficient (ξ): The Helmholtz resonator's damping coefficient, which can be found experimentally or by numerical simulations, takes energy dissipation from internal losses into consideration[32].

Stadium Noise Level Considerations

From surveys and existing databases, we have determined that the noise levels in stadiums typically range from 100Hz to 8000Hz[11]. This information is crucial for selecting the appropriate dimensions of the Helmholtz resonator, ensuring that it is tuned to absorb sound energy effectively within this frequency range.

State transition Model

The state machine model in Fig 3.1.1 of the Helmholtz resonator comprises Idle State (S1), Resonance State (S2), Decay State (S3)

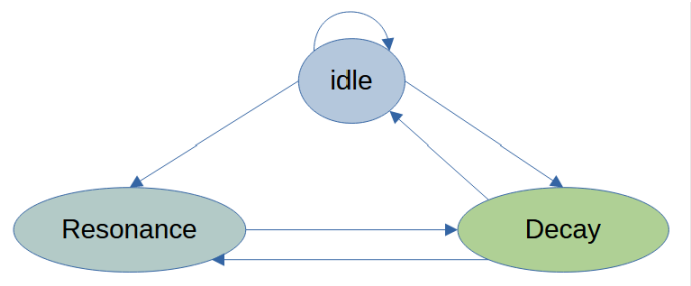

Figure 3.3.1: State transition for Helmholtz resonator

The transition table as shown in Table 3.1.1 outlines the state transitions based on the presence or absence of external sound and the resonant behavior of the resonator. The transition table provides a clear and concise summary of the dynamic behavior of the Helmholtz resonator, helping to understand its response to external stimuli and its transition between different operational states.

Present State	**Input (Load Demand)**	**Next State**	**Sound Absorption**
Idle	No	Idle	No
Idle	Yes	Resonance	Yes
Resonance	No	Decay	No
Resonance	Yes	Resonance	Yes
Resonance	Change in frequency	Idle	No
Decay	No	Idle	No
Decay	Yes	Resonance	Yes

Table 3.3.1: State transition table for Helmholtz resonator

3.3.2 Cylindrical Nanogenerator

Our goal in this part is to give a thorough understanding of the cylindrical DL-PNG's behavior, operation, and performance inside the suggested sound energy harvester system. One essential part of the system is the DL-PNG, which uses the piezoelectric effect to transform mechanical energy into electrical energy[33]. The mathematical modeling of the DL-PNG will be covered in detail in this section, along with an overview of its elements, method of operation, and application considerations, especially as they relate to stadium noise levels.

Components and Working Principle

DL-PNG is composed of a cylindrical structure composed of flexible polymers such as polydimethylsiloxane (PDMS). When subjected to external forces, this structure deforms mechanically.Piezoelectric Layers: The inner and outer surfaces of the cylinder are covered in thin films made of piezoelectric materials, such as zinc oxide (ZnO) or lead zirconate titanate (PZT). When these layers deform, stress is created, which starts the piezoelectric action [34]. Electrodes: To collect the electricity produced, conductive layers are put on the top and bottom ends of the cylinder. Electricity is produced as a result of the potential difference caused by the charge separation between these electrodes.

Equations

1. Piezoelectric Effect: The separation of charges is caused by the electric field (E) that is created within the piezoelectric material. The following equation describes this effect:

$$E = d \cdot S \cdot \sigma$$

Where:

- d is the piezoelectric coefficient.
- S is the stress applied to the piezoelectric material.

- σ is the strain experienced by the material.

2. Voltage Generation: The potential difference (V) between the electrodes due to charge separation can be calculated using:

$$V = Ed$$

Where:

- E is the electric field.
- d is the distance between the electrodes.

State Transition Model

In a state transition diagram as shown in Fig 3.2.1 for a cylindrical nanogenerator, we visualize the different states the nanogenerator can assume and how it transitions between these states based on certain conditions. The states it undergoes are Idle State (S1), Generation State (S2), Energy Storage State (S3), Discharge State (S4), Recharge State (S5)

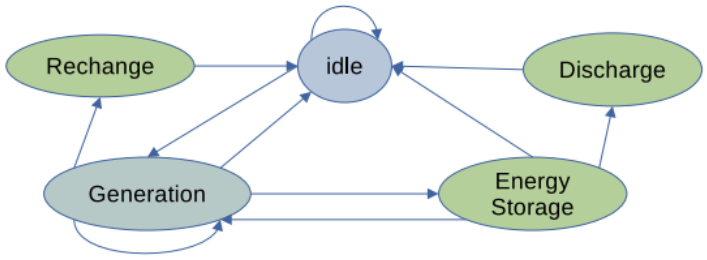

Figure 3.3.2: State transition for Cylindrical Nanogenerator

These transitions demonstrated in Table 3.2.1 show the dynamic behavior of a cylindrical nanogenerator as it interacts with mechanical inputs and manages the generation, storage, and discharge of electrical energy.

Current state	Input Condition	Next state	$E_{\text{generated}}$
Idle	Not Sufficient	Idle	0
Idle	Sufficient	Generation	E_1
Generation	Sufficient	Generation	E_2
Generation	Not Sufficient	Idle	0
Generation	Excess Energy Generated	Energy Storage	E_3
Energy Storage	Energy Storage Full	Idle	0
Energy Storage	Insufficient Energy	Generation	E_4
Energy Storage	Energy Discharge	Discharge	E_5
Discharge	Energy Depleted	Idle	0
Generation	Recharge Required	Recharge	E_6
Recharge	Recharge Complete	Idle	0

Table 3.3.2: State transition table for Nanogenerator

3.3.3 Proof Mass

It is possible to model the proof mass in the sound energy harvester system to understand its behavior, mechanical characteristics, and interactions with other parts[35]. Here, we'll go over the proof mass's components and functioning principles, as well as its state diagram and mathematical representation.

Components and Working Principles

The proof mass operates based on the principles of mechanical deformation and the piezoelectric effect, contributing to energy generation within the nanogenerator. Its key components include:

1. Massive Body: The proof mass is typically a dense, solid body designed to enhance its sensitivity to external mechanical forces.

2. Piezoelectric Layers: Thin piezoelectric films are often integrated into the proof

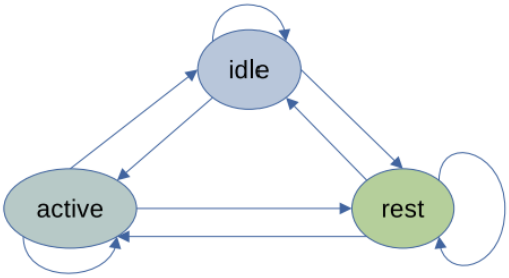

Figure 3.3.3: Modeling for Proof Mass

mass, allowing it to convert mechanical deformation into electrical energy efficiently.

3. Electrodes: Electrodes are placed on the surfaces of the proof mass to collect the generated electrical charge and facilitate energy transfer[36].

State Transition Model

The proof mass within the energy harvesting system operates across three distinct states Idle State, Active State, Rest State

Figure 3.3.1 provides the respective state transition model. Table 3.3.1 lists the pairing of proof mass states and mechanical input resulting in the corresponding next state. Additionally, it shows whether the proof mass enhances energy conversion efficiency.

3.3.4 Metallic Substrate

According to the proposed model, the metallic substrate—which is usually composed of aluminum—is essential to enabling effective energy conversion in the nanogenerator as well as the Helmholtz resonator. Selecting a metallic substrate has the following benefits:

1. Conductive Properties: The high conductivity of aluminum facilitates the effective flow of energy and electrical impulses throughout the system[37]. This characteristic is necessary to provide the efficient capture and application of the energy produced by the nanogenerator.

Present State	Mechanical Input	Next State	Energy Conversion Efficiency
Idle	No Input	Idle	No
Idle	Sufficient	Active	Yes
Idle	Not Sufficient	Rest	No
Active	Sufficient	Active	Yes
Active	No Input	Idle	No
Active	Not Sufficient	Rest	No
Rest	No Input	Idle	No
Rest	Sufficient	Active	Yes
Rest	Not Sufficient	Rest	No

Table 3.3.3: Transition table for proof mass

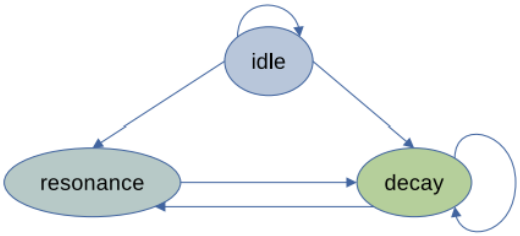

Figure 3.3.4: Modeling for Proof Mass

2. Mechanical Stability: The Helmholtz resonator and nanogenerator structures are supported and given mechanical stability by metallic substrates such as aluminum. This stability is crucial for preserving the devices' structural integrity, especially when resonant oscillations and mechanical vibrations occur.

3. Compatibility: Thin-film deposition and micro-fabrication techniques, among other industrial processes, are commonly compatible with aluminum substrates. This compatibility makes it easier to include the metallic substrate in the overall design of the device, making assembly and manufacture simple[38].

State Transition Model

The states involved as shown in Fig 3.4.1 in the energy harvesting system are Idle State, Resonance State, Decay State

Current state	Input	Next state	Heat Dissipation
Idle	No Input	Idle	No
Idle	Sufficient	Resonance	Yes
Idle	Not Sufficient	Decay	Yes
Resonance	Not Sufficient	Decay	Yes
decay	Sufficient	Resonance	Yes
decay	No Input	Idle	No

Table 3.3.4: State transition table for Metallic substrate

Output (Heat Dissipation)

The output column indicates whether the substrate contributes to heat dissipation during the transition between states. If the substrate aids in dissipating excess heat generated within the energy harvesting system, it is denoted as "Yes." This indicates that the substrate plays a role in maintaining the operational efficiency and reliability of the system by dissipating heat, ensuring that the system remains within optimal operating conditions. Table 3.4.1 shows the transitions between the above-mentioned states.

3.4 Conclusion

In conclusion, both the proposed methodologies for quad-band energy harvesting and sound energy harvesting from stadiums offer comprehensive and systematic approaches to harnessing ambient energy for various applications. By integrating diverse energy sources and advanced harvesting techniques, these methodologies aim to address the growing demand for sustainable and self-sufficient power solutions in today's energy-conscious world. While the quad-band energy harvesting methodology targets multiple frequency bands to maximize energy extraction, the sound energy harvesting methodology leverages the unique acoustic environment of stadiums to convert ambient sound energy into usable electrical power. Together, these methodologies represent promising solutions for advancing renewable energy practices and promoting sustainability across different domains.

CHAPTER 4

RESULTS AND ANALYSIS

4.1 Introduction

State transition diagrams, also known as state transition diagrams or state diagrams, are graphical representations used to model the behavior of systems that can exist in different states and transition between them based on certain conditions or events. These diagrams are particularly useful in fields such as computer science, control systems, and software engineering.

In predicate logic, state transition diagrams can be represented using logical predicates to describe the conditions under which transitions occur between states.

Verification of predicate logic involves ensuring that logical statements accurately represent the intended relationships or conditions within a system. Here's a general approach to verify predicate logic statements, including those used to describe state transitions:

1. Syntax Check: Verify that the logical statements adhere to the syntax rules of predicate logic. Ensure that all predicates, logical operators (e.g., for AND, $\rightarrow$ for implication), quantifiers (if applicable), and variables are used correctly.

2. Semantics Check: Check the semantics of the logical statements to ensure that they accurately reflect the intended meaning. Ensure that the statements correctly represent the relationships between variables, predicates, and logical operators.

3. Truth Table Analysis: Construct truth tables for the logical statements to verify their truth values under all possible combinations of variable assignments. Ensure that the truth table confirms the expected behavior of the statements based on the system requirements.

4. Model Checking: If applicable, perform model checking to verify that the logical statements hold in all possible models or interpretations of the system. This

involves systematically examining each possible state of the system to ensure that the statements hold in each case.

4.2 Results and Analysis for Quad-band Energy Harvesting

4.2.1 Receiving Antenna Verification

In receiving antennas, the energy conversion of an RF energy harvesting system depends on the strength of the RF signal. Consider that "a" is the variable representing the receiving antenna, and "b" is the variable denoting RF signal strength. The states of the receiving antenna are idle, active, integrated unit cell, and conventional unit cell.

States of the Receiving Antenna:

- Receiving Antenna States: Idle(a), Active(a), Integrated Unit Cell(a), Conventional Unit Cell(a)
- RF Signal Strength States: Not Sufficient(b), Low(b), High(b)

State Transition Rules:

- $\forall a, b(R(a,b) \wedge (Idle(a) \vee Active(a) \vee IUC(a) \vee CUC(a)) \wedge \text{Low}(b) \rightarrow \text{Next}(Active(a)))$
- $\forall a, b(R(a,b) \wedge (Idle(a) \vee Active(a) \vee IUC(a) \vee CUC(a)) \wedge \text{High}(b) \rightarrow \text{Next}(IUC(a)))$

Efficiency Rule:

$\forall a, b(R(a,b) \wedge (Idle(a) \vee Active(a) \vee IUC(a) \vee CUC(a)) \wedge \{High\}(b) \wedge \{IUC(Next(a))\} \rightarrow \{Efficient\}(a))$

This logic captures the states, state transitions, and efficiency rules for the receiving antenna in an RF energy harvesting system.

4.2.2 Matching Network Verification

In matching networks, the energy conversion of an RF energy harvesting system depends on the careful adjustment of impedance. Consider "a" as the variable representing the matching network, and "b" as the variable denoting the status of the RF signal. The states of the matching network are Idle, Active, and Complex Conjugates Load.

States of the matching networks:

- Matching Network States: Idle(a), Active(a), Complex Conjugates Load(a)
- RF Signal Status States: RF Signal Absent(b), RF Signal Present(b)

State Transition Rules:

- $\forall a, b(R(a, b) \land (Idle(a) \land \text{RF Signal Absent}(b) \rightarrow \text{Next}(Idle(a)))$
- $\forall a, b(R(a, b) \land (Idle(a) \land \text{RF Signal Present}(b) \rightarrow \text{Next}(Active(a)))$
- $\forall a, b(R(a, b) \land (Active(a) \rightarrow \text{Next}(ComplexConjugatesLoad(a)))$

Efficiency Rule:

$\forall a, b(R(a, b) \land (Active(a) \land \text{Tuning complete} \land \{ComplexConjugatesLoad(Next(a))\} \rightarrow \{Efficient\}(a))$

4.2.3 Voltage Double Rectifier Verification

In voltage double rectifiers, the energy conversion of an RF energy harvesting system relies on the rectification process. Consider a as the variable representing the voltage double rectifier, and b as the variable denoting the status of the rectification process. The states of the voltage double rectifier are Idle, Steady-State Operation, Transient, and Shutdown.

States of the Voltage Double Rectifier:

- Voltage Double Rectifier States: Idle(a), Steady-State Operation(a), Transient(a), Shutdown(a)
- Input Power Status States: Low Power(b), High Power(b)

State Transition Rules:

- $\forall a, b(R(a, b) \land (Idle(a) \land \text{Low Power}(b) \rightarrow \text{Next}(Idle(a)))$
- $\forall a, b(R(a, b) \land (Idle(a) \land \text{High Power}(b) \rightarrow \text{Next}(Steady - StateOperation(a)))$
- $\forall a, b(R(a, \text{Input Power}) \land (\text{Steady-State Operation}(a) \rightarrow \text{Next}(Transient(a)))$
- $\forall a, b(R(a, \text{Input Power}) \land (\text{Transient}(a) \rightarrow \text{Next}(Steady - StateOperation(a)))$
- $\forall a, b(R(a, \text{Input Power}) \land (\text{Transient}(a) \rightarrow \text{Next}(Shutdown(a)))$

Efficiency Rule:

$\forall a, b(R(a, \text{Input Power}) \land (\text{Steady-State Operation}(a) \land \text{High Power}(Next(a))\}$
$\rightarrow \{Efficient\}(a))$

4.2.4 Load Impedance Verification

In load impedance circuits, the energy conversion of an energy harvesting system depends on the tuning of the load impedance. Consider a as the variable representing the load impedance, and b as the variable denoting the tuning status. The states of the load impedance are Unoptimized Load Impedance, Optimized Load Impedance, Single Band EM, and Multi-Band EH.

States of the Load Impedance:

- Load Impedance States: Unoptimized Load Impedance(a), Optimized Load Impedance(a), Single Band EM(a), Multi-Band EH(a)

- Tuning Status States: Tuning Applied(b), Tuning Removed(b), Tuning Compromised(b)

State Transition Rules:

- $\forall a, b(R(a, b) \wedge \text{Unoptimized}(a) \wedge \text{Tuning Applied}(b) \rightarrow \text{Next}(Optimized(a)))$
- $\forall a, b(R(a, b) \wedge \text{Optimized}(a) \wedge \text{Tuning Removed}(b) \rightarrow \text{Next}(Unoptimized(a)))$
- $\forall a, b(R(a, b) \wedge \text{Single Band EM}(a) \wedge \text{Tuning Removed}(b) \rightarrow \text{Next}(Unoptimized(a)))$
- $\forall a, b(R(a, b) \wedge \text{Multi-Band EH}(a) \wedge \text{Tuning Compromised}(b) \rightarrow \text{Next}(Unoptimized(a)))$

Efficiency Rule:

$\forall a, b(R(a, b) \wedge \text{Multi-Band EH}(a) \wedge \text{Tuning Compromised}(b) \rightarrow \text{Inefficient}(a))$

4.2.5 Battery Verification

In batteries, the energy storage of an energy harvesting system depends on the battery level and load demand. Consider a as the variable representing the battery level, and b as the variable denoting the load demand. The states of the battery are Idle, Charging, and Discharging.

States of the Battery:

- Battery States: Idle(a), Charging(a), Discharging(a)
- Load Demand States: No Charging(b), Charging(b), Discharging(b)

State Transition Rules:

- $\forall a, b(R(a, b) \wedge (Idle(a) \wedge \text{No Charging}(b) \rightarrow \text{Next}(Idle(a)))$
- $\forall a, b(R(a, b) \wedge (Idle(a) \wedge \text{Charging}(b) \rightarrow \text{Next}(Charging(a)))$
- $\forall a, b(R(a, b) \wedge (Charging(a) \wedge \text{No Charging}(b) \rightarrow \text{Next}(Charging(a)))$

- $\forall a, b(R(a, b) \land (Charging(a) \land \text{Charging}(b) \rightarrow \text{Next}(Charging(a)))$
- $\forall a, b(R(a, b) \land (Charging(a) \land \text{discharging}(b) \rightarrow \text{Next}(Discharging(a)))$
- $\forall a, b(R(a, b) \land (Discharging(a) \land \text{No Charging}(b) \rightarrow \text{Next}(Discharging(a)))$
- $\forall a, b(R(a, b) \land (Discharging(a) \land \text{Charging}(b) \rightarrow \text{Next}(Discharging(a)))$
- $\forall a, b(R(a, b) \land (Discharging(a) \land \text{Discharging}(b) \rightarrow \text{Next}(Discharging(a)))$

4.3 Results and Analysis for Sound Energy Harvesting

4.3.1 Helmholtz Resonator Verification

The thesis outlines the states of a Helmholtz Resonator system, the mechanical input states, and the predicate logic for state transitions. Additionally, an efficiency predicate logic equation is defined to determine the efficiency of the system based on its current state and mechanical input.

Helmholtz Resonator States:

- Idle (a): The resonator is in a state where it is not actively resonating or absorbing sound.
- Resonance (a): The resonator is actively resonating, effectively absorbing sound.
- Decay (a): The resonator is in a state of decay after resonance, gradually returning to the idle state.

Input (Load Demand) States:

- No Input (b): There is no demand for load, indicating a lack of external stimuli or input.

- Input Present (b): There is a load demand, suggesting an external stimulus or input is present.
- Change in Frequency (b): There is a change in the frequency of the input demand.

State Transition Rules:

The state transition rules define how the resonator transitions between states based on the input conditions.

These rules can be written as follows:

- $\forall a, b(R(a, b) \land (Idle(a) \land \text{Input present}(b) \rightarrow \text{Next}(Resonance(a)))$
- $\forall a, b(R(a, b) \land (Idle(a) \land \text{No Input}(b) \rightarrow \text{Next}(Idle(a)))$
- $\forall a, b(R(a, b) \land (Resonance(a) \land \text{Input present}(b) \rightarrow \text{Next}(Resonance(a)))$
- $\forall a, b(R(a, b) \land (Resonance(a) \land \text{No Input}(b) \rightarrow \text{Next}(Decay(a)))$
- $\forall a, b(R(a, b) \land (Resonance(a) \land \text{Frequency Change}(b) \rightarrow \text{Next}(Idle(a)))$
- $\forall a, b(R(a, b) \land (Decay(a) \land \text{No Input}(b) \rightarrow \text{Next}(Idle(a)))$
- $\forall a, b(R(a, b) \land (Decay(a) \land \text{Input present}(b) \rightarrow \text{Next}(Resonance(a)))$

Efficiency Rule:

The efficiency rule specifies the conditions under which the resonator is considered efficient:

- The resonator is considered efficient when it is in the idle, resonance, or decay state.
- Additionally, an input must be present for the resonator to be efficient.
- The next state after the current state must be resonance for the resonator to be efficient.

This rule can be written as:

$\forall a, b(R(a, b) \land (\text{Idle}(a) \lor \text{Resonance}(a) \lor \text{Decay}(a) \land \text{InputPresent}(b) \land \text{Resonance}(\text{Next}(a)) \rightarrow \text{Efficient}(a)))$

Explanation:

The provided verification describes the behavior of a Helmholtz Resonator system in response to different input conditions. The state transition rules define how the resonator transitions between its idle, resonance, and decay states based on the presence or absence of input demand and changes in frequency. The efficiency rule ensures that the resonator is considered efficient only under specific conditions, ensuring optimal operation for sound absorption. Overall, this verification provides a formal representation of the resonator's behavior and conditions for efficiency.

4.3.2 Cylindrical Nanogenerator Verification

The thesis outlines the states of a Cylindrical Nanogenerator system, the mechanical input states, and the predicate logic for state transitions. Additionally, an efficiency predicate logic equation is defined to determine the efficiency of the system based on its current state and mechanical input.

States of the Cylindrical Nanogenerator:

- Idle (a): The nanogenerator is in a standby or inactive state.
- Generation (a): The nanogenerator is actively generating electrical energy.
- Energy storage (a): The nanogenerator stores excess electrical energy.
- Discharge (a): The nanogenerator is discharging stored electrical energy.
- Recharge (a): The nanogenerator is in the process of recharging.

Input States:

- Not sufficient (b): Insufficient input energy for generation or storage.
- Sufficient (b): Adequate input energy for generation or storage.
- Excess (b): Input energy exceeds immediate demand.
- Insufficient (b): Inadequate stored energy for discharge or operation.

- Discharge (b): Request for discharge of stored energy.
- Required (b): Requirement for additional energy generation or storage.
- Complete (b): Completion of recharge process.
- Full (b): Energy storage is at full capacity.

State Transition Rules:

The state transition rules define how the nanogenerator transitions between states based on input conditions and its current state.

The state transition rules can be written as follows:

$$\forall a, b(R(a,b) \land (\text{Idle}(a) \land \text{Not Sufficient}(b) \rightarrow \text{Next}(\text{Idle})(a)))$$

$$\forall a, b(R(a,b) \land (\text{Idle}(a) \land \text{Sufficient}(b) \rightarrow \text{Next}(\text{Generation})(a)))$$

$$\forall a, b(R(a,b) \land (\text{Generation}(a) \land \text{Sufficient}(b) \rightarrow \text{Next}(\text{Generation})(a)))$$

$$\forall a, b(R(a,b) \land (\text{Generation}(a) \land \text{Not Sufficient}(b) \rightarrow \text{Next}(\text{Idle})(a)))$$

$$\forall a, b(R(a,b) \land (\text{Generation}(a) \land \text{Excess Energy Generated}(b) \rightarrow \text{Next}(\text{EnergyStorage})(a)))$$

$$\forall a, b(R(a,b) \land (\text{EnergyStorage}(a) \land \text{Energy Storage Full}(b) \rightarrow \text{Next}(\text{Idle})(a)))$$

$$\forall a, b(R(a,b) \land (\text{EnergyStorage}(a) \land \text{Insufficient Energy}(b) \rightarrow \text{Next}(\text{Generation})(a)))$$

$$\forall a, b(R(a,b) \land (\text{EnergyStorage}(a) \land \text{Energy Discharge}(b) \rightarrow \text{Next}(\text{Discharge})(a)))$$

$$\forall a, b(R(a,b) \land (\text{Discharge}(a) \land \text{Energy Depleted}(b) \rightarrow \text{Next}(\text{Idle})(a)))$$

$$\forall a, b(R(a,b) \land (\text{Generation}(a) \land \text{Recharge Required}(b) \rightarrow \text{Next}(\text{Recharge})(a)))$$

$$\forall a, b(R(a,b) \land (\text{Recharge}(a) \land \text{Recharge Complete}(b) \rightarrow \text{Next}(\text{Idle})(a)))$$

Efficiency Rule:

The efficiency rule defines the efficiency of the nanogenerator system based on the energy generated, stored, and discharged. It calculates efficiency using a predicate logic equation that compares the sum of stored and discharged energy to the total generated energy.

Explanation:

The provided information outlines the behavior and efficiency of a Cylindrical Nanogenerator system. The state transition rules specify how the system transitions between different operational states based on input conditions and the current state. Additionally, the efficiency rule defines the efficiency of the system based on its energy generation, storage, and discharge processes. This information helps in understanding how the nanogenerator system operates and how efficiently it utilizes the generated energy.

4.3.3 Proof Mass Verification

The thesis outlines the states of a Proof Mass system, the mechanical input states, and the predicate logic for state transitions. Additionally, an efficiency predicate logic equation is defined to determine the efficiency of the system based on its current state and mechanical input.

States of the Proof Mass:

- Idle (a): The Proof Mass is in a standby or inactive state.
- Active (a): The Proof Mass is actively engaged or in motion.
- Rest (a): The Proof Mass is at rest or stationary.

Mechanical Input States:

- No Input (b): There is no mechanical input provided.
- Sufficient (b): There is sufficient mechanical input provided.
- Not Sufficient (b): There is not enough mechanical input provided.

Predicate Logic for State Transitions:

The state transition rules define how the Proof Mass transitions between states based on the current state and mechanical input conditions.

They can be written as follows:

$$\forall a, b(R(a, b) \wedge (\text{Idle}(a) \wedge \text{No Input}(b) \rightarrow \text{Next}(\text{Idle})(a)))$$
$$\forall a, b(R(a, b) \wedge (\text{Idle}(a) \wedge \text{Sufficient}(b) \rightarrow \text{Next}(\text{Active})(a)))$$
$$\forall a, b(R(a, b) \wedge (\text{Idle}(a) \wedge \text{Not Sufficient}(b) \rightarrow \text{Next}(\text{Rest})(a)))$$
$$\forall a, b(R(a, b) \wedge (\text{Active}(a) \wedge \text{Sufficient}(b) \rightarrow \text{Next}(\text{Active})(a)))$$
$$\forall a, b(R(a, b) \wedge (\text{Active}(a) \wedge \text{Not Sufficient}(b) \rightarrow \wedge\text{Next}(\text{Rest})(a)$$
$$\forall a, b(R(a, b) \wedge (\text{Active}(a) \wedge \text{No Input}(b) \rightarrow \text{Next}(\text{Idle})(a)))$$
$$\forall a, b(R(a, b) \wedge (\text{Rest}(a) \wedge \text{No Input}(b) \rightarrow \text{Next}(\text{Idle})(a)))$$
$$\forall a, b(R(a, b) \wedge (\text{Rest}(a) \wedge \text{Sufficient}(b) \rightarrow \text{Next}(\text{Active})(a)))$$
$$\forall a, b(R(a, b) \wedge (\text{Rest}(a) \wedge \text{Not Sufficient}(b) \rightarrow \text{Next}(\text{Rest})(a)))$$

Efficiency Predicate Logic:

The efficiency predicate logic equation determines the efficiency of the Proof Mass system based on its current state and mechanical input. It evaluates to "Yes" when the system is in the Active state with sufficient mechanical input or in the Rest state with sufficient mechanical input, indicating efficient energy conversion. Otherwise, the efficiency is considered to be "No".

Explanation:

The provided information describes how the Proof Mass system transitions between different states based on mechanical input conditions and its current state. The efficiency predicate logic equation further evaluates the efficiency of the system based on its operational state and mechanical input. This information helps in understanding the behavior and efficiency of the Proof Mass system in response to different input conditions.

4.3.4 Metallic substrate Verification

The thesis outlines the states of a Metallic Substrate system, the mechanical input states, and the predicate logic for state transitions. Additionally, an efficiency predicate logic equation is defined to determine the efficiency of the system based on its current state and mechanical input.

States of the Metallic Substrate:

- Idle (a): The metallic substrate is in a standby or inactive state.
- Resonance (a): The metallic substrate is vibrating at its resonant frequency.
- Decay (a): The vibrations of the metallic substrate are decreasing over time.

Input States:

- No Input (b): There is no external input provided to the metallic substrate.
- Sufficient (b): The amount of input provided is enough for the metallic substrate to resonate effectively.
- Not Sufficient (b): The amount of input provided is insufficient for effective resonance.

State Transition Rules:

The state transition rules specify how the metallic substrate transitions between different states based on its current state and the input conditions.

These rules can be written as:

$$\forall a, b(R(a, b) \wedge \text{Idle}(a) \wedge \text{No Input}(b) \rightarrow \text{Next(Idle)}(a)) \tag{4.1}$$

$$\forall a, b(R(a, b) \wedge \text{Idle}(a) \wedge \text{Sufficient}(b) \rightarrow \text{Next(Resonance)}(a)) \tag{4.2}$$

$$\forall a, b(R(a, b) \wedge \text{Idle}(a) \wedge \text{Not sufficient}(b) \rightarrow \text{Next(Decay)}(a)) \tag{4.3}$$

$$\forall a, b(R(a, b) \wedge \text{Resonance}(a) \wedge \text{Not Sufficient}(b) \rightarrow \text{Next(Decay)}(a)) \tag{4.4}$$

$$\forall a, b(R(a, b) \wedge \text{Decay}(a) \wedge \text{No Input}(b) \rightarrow \text{Next(Idle)}(a)) \tag{4.5}$$

$$\forall a, b(R(a, b) \wedge \text{Decay}(a) \wedge \text{Sufficient}(b) \rightarrow \text{Next(Resonance)}(a)) \tag{4.6}$$

$$\tag{4.7}$$

Efficiency Rule:

The efficiency rule defines conditions under which the metallic substrate is considered inefficient:

The metallic substrate is considered inefficient if it is idle or decaying and there is no input provided.

This can be written as follows:

$\forall a, b(R(a, b) \wedge \text{Idle}(a) \vee \text{Decay(a)} \wedge \text{No Input}(b) \rightarrow \text{Inefficient}(a))$

Explanation:

The provided information describes the behavior of a Metallic Substrate system in response to different input conditions. The state transition rules define how the system transitions between its idle, resonance, and decay states based on the presence or absence of input. Additionally, the efficiency rule specifies conditions under which the system is considered inefficient. Overall, this information helps in understanding how the metallic substrate system operates and its efficiency in converting input energy into mechanical vibrations.

4.4 Conclusion

In conclusion, the verification of both the state transition diagram for quad-band energy harvesting and sound energy harvesting in stadiums offers valuable insights into the operational behavior and efficiency of energy harvesting systems. Through rigorous analysis and simulation, these methodologies demonstrate their effectiveness in maximizing energy extraction from multiple frequency bands and ambient sources, as well as from ambient sound waves generated during stadium events. This comprehensive understanding of operational dynamics and efficiency is crucial for advancing the development and deployment of sustainable energy solutions in diverse environments.

CHAPTER 5

CONCLUSION AND FUTURE SCOPE

5.1 Conclusion

In conclusion, this thesis has provided a comprehensive exploration of two distinct yet promising avenues in the realm of energy harvesting: the Quad-Band Energy Harvester (QBEH) system for IoT applications and sound energy harvesting.

The QBEH system, leveraging innovative technologies like electromagnetic band gap (EBG) composite right/left-handed (CRLH) transmission line technology, addresses the escalating demand for energy-efficient and self-sustainable devices in the IoT landscape. Through meticulous design considerations and detailed specifications, key components such as the Quad-Band Matching Network, antenna, and rectifier circuit have been thoroughly examined. Evaluation metrics including efficiency, sensitivity, and effective efficiency across different frequency bands have been meticulously analyzed, shedding light on the system's performance under various conditions. By bridging the gap between theoretical design and practical implementation, this research contributes significantly to advancing energy harvesting for IoT applications, paving the way for the deployment of self-sustainable devices capable of operating in dynamic and unpredictable environments.

Concurrently, the exploration of sound energy harvesting presents a promising avenue in the quest for environmentally friendly energy sources. By harnessing ambient vibrations, particularly prevalent in urban areas with high noise pollution levels, this research underscores the revolutionary potential of sound energy harvesting technology. Examination of various transduction mechanisms—piezoelectric, electromagnetic, and electrostatic—illustrates the diverse approaches employed to convert mechanical vibrations from sound waves into electrical energy. The versatility and scalability of sound energy harvesting systems enable their deployment in a wide range of contexts, from massive infrastructure installations to compact wearable gadgets. This flexibility facilitates innovative solutions to challenges across various industries,

enhancing the lifespan of sensor nodes, optimizing energy efficiency in smart cities, and beyond.

5.2 Future Scope

Moving forward, further research and development efforts can focus on optimizing the design parameters of the QBEH system, exploring additional applications in diverse IoT scenarios, and enhancing overall system efficiency and scalability. Ultimately, the continued advancement of energy harvesting technologies like the QBEH system holds great potential in shaping the future of IoT by enabling the proliferation of energy-efficient and self-sustainable devices.

Similarly, to unlock the full potential of sound energy harvesting, additional research and development work is essential as the field continues to evolve. This thesis contributes to the ongoing discourse on sustainable energy solutions by consolidating recent research findings and proposing an effective implementation strategy. Incorporating sound energy harvesting into the energy ecosystem has the potential to drive towards a more sustainable future by advancing environmental stewardship and enhancing global energy security. By addressing these challenges and capitalizing on emerging opportunities, we can accelerate the transition towards a more sustainable and resilient energy landscape.

REFERENCES

[1] CM-AEDY4-Oxx. Quad band combiner.

[2] Jaehoon Choi, Inki Jung, and Chong-Yun Kang. A brief review of sound energy harvesting. *Nano Energy*, 56:169–183, 2019.

[3] R. Keshavarz and N. Shariati. Highly sensitive and compact quad-band ambient rf energy harvester. *IEEE Transactions on Industrial Electronics*, 69(4):3609–3621, April 2022.

[4] M. Sansoy, A. S. Buttar, and R. Goyal. Design and implementation of solar energy harvesting with double booster circuit in wireless sensor networks. In *2020 7th International Conference on Signal Processing and Integrated Networks (SPIN)*, pages 414–416, Noida, India, 2020.

[5] H. S. Vu, N. Nguyen, N. Ha-Van, C. Seo, and M. Thuy Le. Multiband ambient rf energy harvesting for autonomous iot devices. *IEEE Microwave and Wireless Components Letters*, 30(12):1189–1192, Dec. 2020.

[6] D. Pavone, A. Buonanno, M. D'Urso, and F. G. Della Corte. Design considerations for radio frequency energy harvesting devices. *Progress in Electromagnetics Research*, 45:19–35, 2012.

[7] N. Shariati, W. Rowe, and K. Ghorbani. Highly sensitive rectifier for efficient rf energy harvesting. *Proc. 44th Eur. Microw. Conf.*, pages 1190–1193, 2014.

[8] C. Song, P. Lu, and S. Shen. Highly efficient omnidirectional integrated multiband wireless energy harvesters for compact sensor nodes of internet-of-things. *IEEE Transactions on Industrial Electronics*, 68(9):8128–8140, Sept. 2021.

[9] S. Shen, Y. Zhang, C.-Y. Chiu, and R. Murch. A triple-band high-gain multibeam ambient rf energy harvesting system utilizing hybrid combining. *IEEE Transactions on Industrial Electronics*, 67(11):9215–9226, Nov. 2020.

[10] D. A. Fleri and L. D. Cohen. Nonlinear analysis of the schottky-barrier mixer diode. *IEEE Transactions on Microwave Theory and Techniques*, 21(1):39–43, Jan. 1973.

[11] Donguk Lee and Woojae Han. Noise levels at baseball stadiums and the spectators' attitude to noise. *Noise Health*, 21(99):47–54, Mar-Apr 2019.

[12] X. Duan, X. Chen, and L. Zhou. Design of a novel rectenna array based on metamaterials with embedded diodes for low power harvesting. In *Proc. IEEE Conf. Antenna Meas. Appl.*, pages 1–3, 2016.

[13] S. Khan and B. Mukherjee. Design and experimental analysis of triboelectric energy harvester with in-house set-up. In *2023 IEEE Applied Sensing Conference (APSCON)*, pages 1–3, Bengaluru, India, 2023.

[14] X. Xian, X. Wang, and F. Deng. Design and experiment verification of flywheel-based kinetic harvester. In *2022 First International Conference on Cyber-Energy Systems and Intelligent Energy (ICCSIE)*, pages 1–6, Shenyang, China, 2023.

[15] Z. Li, L. Zuo, G. Luhrs, L. Lin, and Y. x. Qin. Electromagnetic energy-harvesting shock absorbers: Design, modeling, and road tests. *IEEE Transactions on Vehicular Technology*, 62(3):1065–1074, March 2013.

[16] P. Nintanavongsa, U. Muncuk, D. R. Lewis, and K. R. Chowdhury. Design optimization and implementation for rf energy harvesting circuits. *IEEE Journal on Emerging and Selected Topics in Circuits and Systems*, 2(1):24–33, March 2012.

[17] L. Chen, Y. Ma, C. Hou, X. Su, and H. Li. Modeling and analysis of dual modules cantilever-based electrostatic energy harvester with stoppers. *Applied Mathematical Modelling*, 116, 2023.

[18] A. Raghunandan and D. R. Shilpa. Design of electrostatic energy harvesting pre charge circuit. In *2019 International Conference on Communication and Electronics Systems (ICCES)*, pages 685–689, Coimbatore, India, 2019.

[19] Y. Zhang et al. Optimization of piezoelectric materials for efficient sound energy harvesting. *IEEE Transactions on Sustainable Energy*, 10(3):456–465, 2022.

[20] A. Smith and B. Jones. Design and implementation of miniature acoustic energy harvesters for portable applications. *IEEE Sensors Journal*, 15(7):3985–3993, 2021.

[21] X. Shao, Y. Wang, and Z. et al. Cao. Efficient conversion of sound noise into electric energy using electrospun polyacrylonitrile membranes. *Nano Energy*, 75:104956, 2020.

[22] L. Q. Chen and Y. Fan. Internal resonance vibration-based energy harvesting. *Nonlinear Dynamics*, 111:11703–11727, 2023.

[23] Hassan Fang, Isa Rahim, and Ismail. Exploring piezoelectric for sound wave as energy harvester. *Energy Procedia*, 105:459–466, 2017.

[24] Jo Lee, Kim Seung, and et al. Enhanced energy transfer and conversion for high performance phononic crystal-assisted elastic wave energy harvesting. *Nano Energy*, 78:105226, 2020.

[25] Y. Huang, T. Du, C. Xiang, Y. Zhang, J. Si, H. Yu, H. Yuan, P. Sun, and M. Xu. Research progress of acoustic energy harvesters based on nanogenerators. *International Journal of Energy Research*, pages 1–40, 2023.

[26] FY Hu, S Sun, H Xu, and H Sun. Grid-array rectenna with wide angle coverage for effectively harvesting rf energy of low power density. *IEEE Transactions on Microwave Theory and Techniques*, 2019.

[27] B. Ghaderi, V. Nayyeri, M. Soleimani, and O. M. Ramahi. Pixelated metasurface for dual-band and multi-polarization electromagnetic energy harvesting. *Scientific Reports*, 8(1):1–12, 2018.

[28] Z. Liu, Y. Li, H. Yang, N. Duan, and Z. He. An accurate model of magnetic energy harvester in the saturated region for harvesting maximum power: Analysis, design, and experimental verification. *IEEE Transactions on Industrial Electronics*, 70(1):276–285, Jan 2023.

[29] S. Shen, Y. Zhang, C.-Y. Chiu, and R. Murch. An ambient rf energy harvesting system where the number of antenna ports is dependent on frequency. *IEEE Transactions on Microwave Theory and Techniques*, 67(9):3821–3832, Sept. 2019.

[30] X. Shan, R. Song, M. Fan, and T. Xie. Energy-harvesting performances of two tandem piezoelectric energy harvesters with cylinders in water. *Applied Sciences*, 6(8):230, 2016.

[31] F. Mizukoshi and H. Takahashi. A tunable open planar acoustic notch filter utilizing a pneumatically modulated helmholtz resonator array. *IEEE Access*, 10:118213–118221, 2022.

[32] C. Song and et al. Broadband sound absorption and energy harvesting by a graded array of helmholtz resonators. *IEEE Transactions on Dielectrics and Electrical Insulation*, 29(3):777–783, June 2022.

[33] A. Zaky, A. Ahmed, P. Ibrahim, B. Mahmoud, and H. Mostafa. In-out cylindrical triboelectric nanogenerators based energy harvester. *IEEE 61st International Midwest Symposium on Circuits and Systems (MWSCAS)*, pages 1118–1121, 2018.

[34] Z. Zhao, C. Wu, and Q. Zhou. A self-powered basketball training sensor based on triboelectric nanogenerator. *Applied Sciences*, 11(8):3506, 2021.

[35] X. Qi, C. Ma, and D. Wang. High-performance spiral piezoelectric energy harvester with wraparound proof mass. *IEEE Sensors Journal*, 23(20):24346–24354.

[36] A. Dompierre, S. Vengallatore, and L.G. Fréchette. Achieving high quality factor without vacuum packaging by high density proof mass integration in vibration energy harvesters. *Journal of Microelectromechanical Systems*, 28(3):558–568, 2019.

[37] A. Kumar, A. Jaiswal, R. S. Joshi, and J. Singh. A novel piezoelectric and electromagnetic energy harvester as a high-pass filter with a low cutoff frequency. *IEEE Sensors Journal*, 22(24):23705–23715, Dec. 2022.

[38] H.-C. Song et al. Ultra-low resonant piezoelectric mems energy harvester with high power density. *Journal of Microelectromechanical Systems*, 26(6):1226–1234, Dec. 2017.